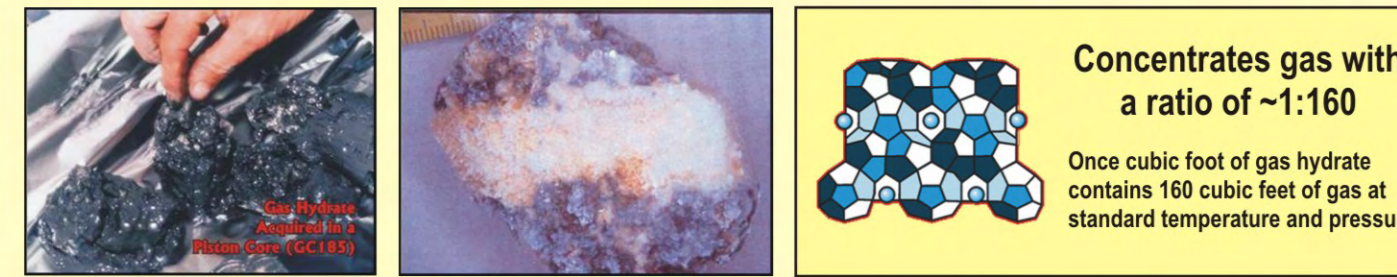


LATE PLEISTOCENE SHELF-EDGE DELTAS AND GROWTH FAULTING IN THE NORTHEAST GULF OF MEXICO: THE EARLY DEVELOPMENT OF SHELF MARGIN RESERVOIR SYSTEMS

GAS HYDRATE

Cagelike Ice Crystal In Which Gas Molecules (Usually Methane) Are Trapped

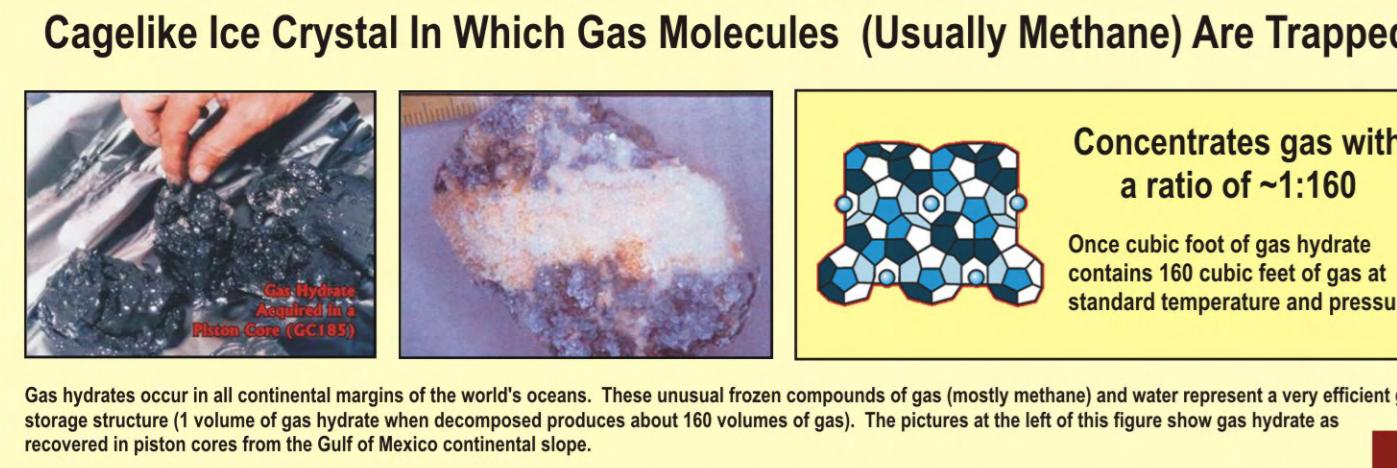


Concentrates gas with a ratio of ~1:160

Once cubic foot of gas hydrate contains 160 cubic feet of gas at standard temperature and pressure.

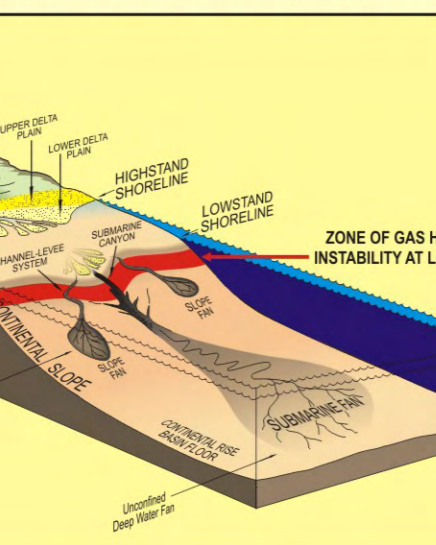
Gas hydrates occur in all continental margins of the world's oceans. These unusual frozen compounds of gas (mostly methane) and water represent a very efficient gas storage structure (1 volume of gas hydrate when decomposed produces about 160 volumes of gas). The pictures at the left of this figure show gas hydrate as recovered in piston cores from the Gulf of Mexico continental slope.

CONTINENTAL MARGIN GAS HYDRATE STABILITY



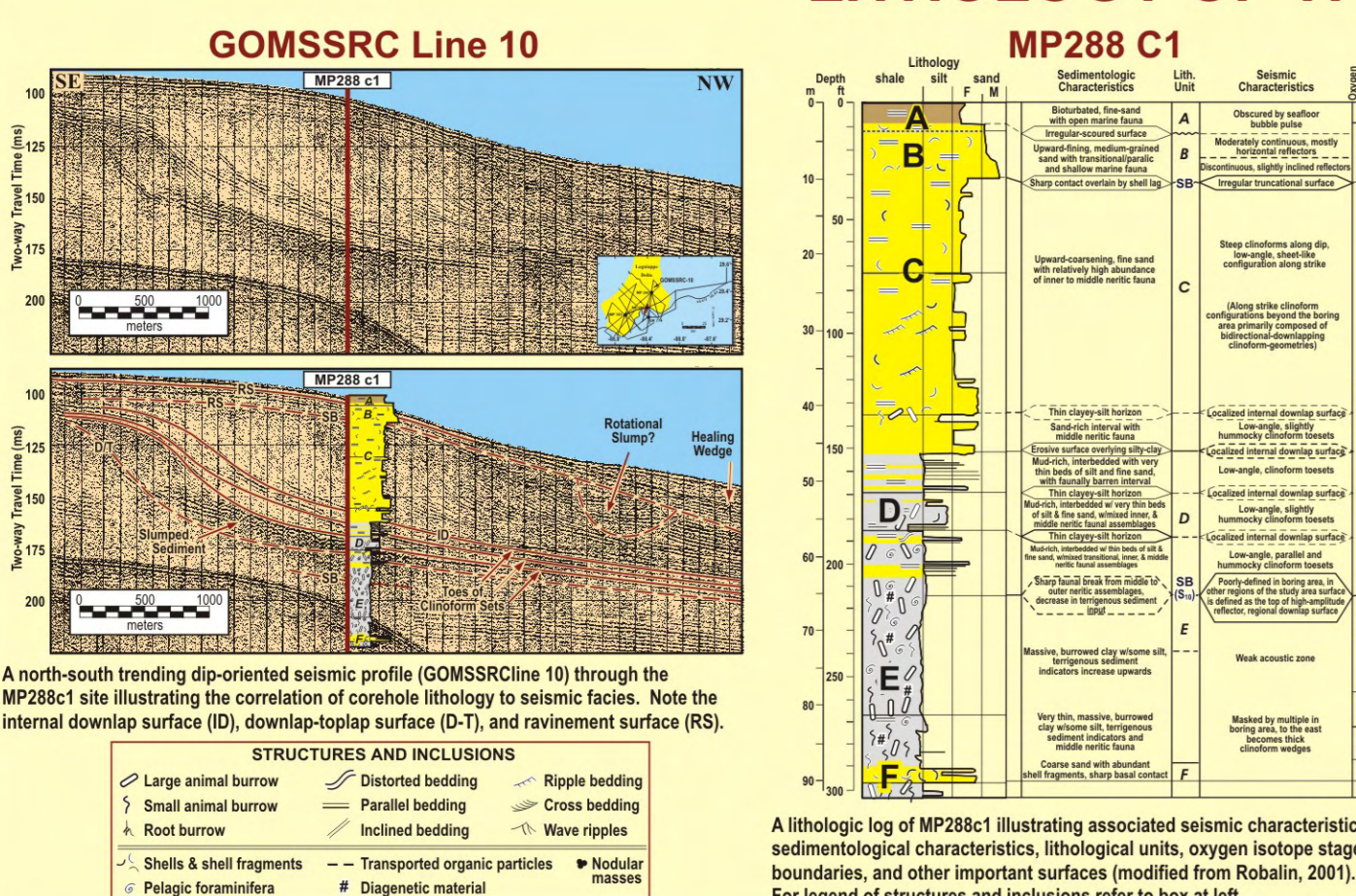
This diagram illustrates the theoretical thickness of the gas hydrate stability zone in continental margins as determined by water depth (hydrostatic pressure), water temperature, the geothermal gradient, and gas composition. At sea level lowstands as occurred at the Latest Pleistocene glacial maximum, the red zone represents zone of the upper continental slope gas hydrates that would decompose. This process produces large volumes of methane that are transferred to the water column and atmosphere. Sediment instability leading to a large-scale shelf-edge submarine landslides is a by-product of gas hydrate decomposition.

ISOPACH



This schematic diagram illustrates the seaward displacement of a fluvial and deltaic deposition system to the shelf-edge accompanying a lowering of sea level as occurred many times during the Pleistocene. Note the zone of the upper continental slope where gas hydrate deposits become unstable because of a reduction of hydrostatic pressure and an increase in water temperature. Slope failures leading to canyon formation can occur. Slumps and density underflows feed slope and deep basin floor fans.

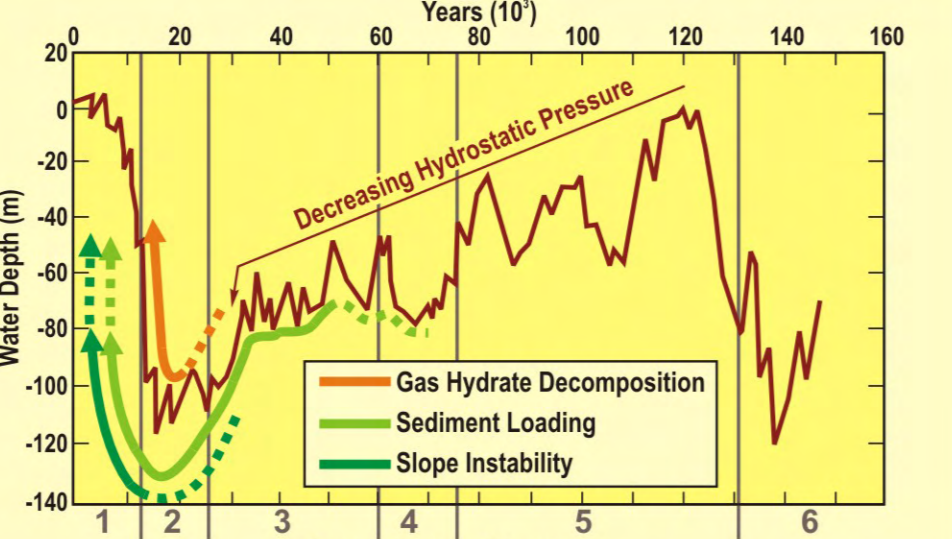
LITHOLOGY OF THE LAGNIAPPE DELTA



UNIT A/B: X-ray radiographs of selected cores from lithologic units A and B in MP288C1. Each picture is a reproduction of the X-ray radiograph negative. Light tones represent areas or features that are dense to the penetration of X-rays. Unit B is represented by high-angle foreset laminations containing abundant abraded shell fragments (radiographs c and d). These shell-rich deposits are overlain by horizontally bedded fine sand (radiograph b). Unit A represents deposition at or near the modern seafloor. Radiograph is a highly burrowed and shell-rich sediment composed mostly of silt and fine sand. This radiograph is typical of sediments near the sediment-water interface at the MP288C1 site.

UNIT C: X-ray radiographs of selected cores from lithologic unit C in MP288C1. Each picture is a reproduction of the X-ray radiograph negative. Light tones represent areas or features that are dense to the penetration of X-rays. The major clinoform set represented by unit C is sand-rich throughout. Massive and parallel-horizontal bedding is most common and represented by all the radiographs of this figure. Shell content increases stratigraphically upward, and oriented shell fabrics are observed near the top of the unit (radiographs a and b). Transported organic particles are missing as discrete layers in unit C. Note the numerous shell fragments scattered throughout each core sample. All cores are 7.6 cm in diameter.

UNIT D: X-ray radiographs of selected cores from lithologic unit D in MP288C1. Each picture is a reproduction of the X-ray radiograph negative. Light tones represent areas or features that are dense to X-rays. These radiographs are typical of the interbedded silty clays, silts, and fine sands that characterize unit D. The shales contain pyritized thin burrows (radiograph a) and nodular diagenetic masses that appear to be confined to burrows (radiograph e). Sands and silts are represented in this lithologic unit as intervals of deformed and convoluted bedding as well as normally graded intervals that overlie shales (radiographs b, c, and d). On seismic profiles unit D is composed of the toes of upslope clinoform sets. Sediment gravity flows and slumping from prograding upslope deltas account for graded and deformed intervals. Each core is 7.6 cm in diameter.

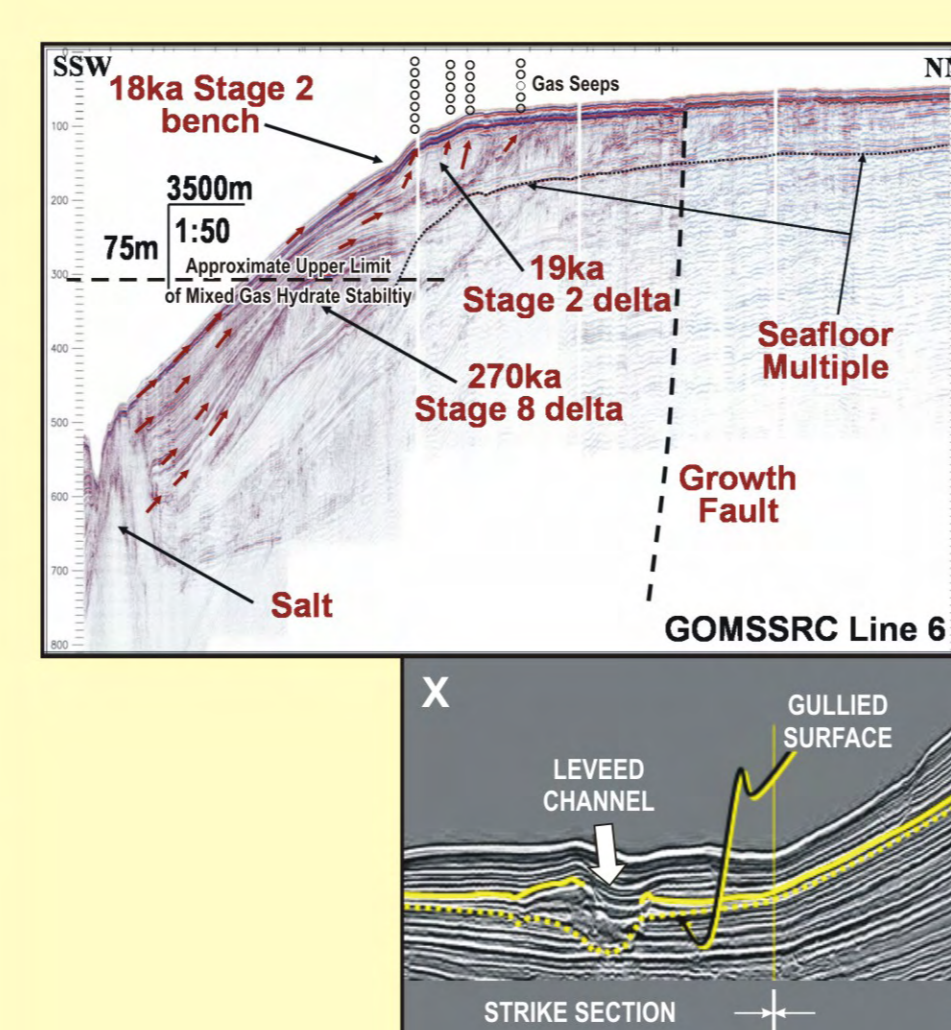


These two curves derived from oxygen isotope data (Shackleton, 1987; Labeyrie et al., 1987) are proxies for eustatic sea level change over the last 140 ka. As sea level falls from the sea highstand approximately 120 ka BP, sources of fluvial sediment move closer to the shelf-edge and certainly impact the shelf-edge and slope as they approach the latest glacial maximum (~18 ka BP). When sea level nears the glacial maximum, sedimentary loading occurs at the shelf-edge and upper slope. At the same time, gas hydrate deposits that were stable at higher sea level positions start to decompose because of decreasing hydrostatic pressure and thermal loading from warm surface waters. Gas released from decomposing hydrates is released in the sediment column, to water column, and to the atmosphere. Sediment instability of the slope and shelf-edge occurs from this hydrate decomposition. Sedimentologically, the result is sediment by-passing to deep water by small slumps to massive shelf edge evacuations that result in submarine canyon formation.

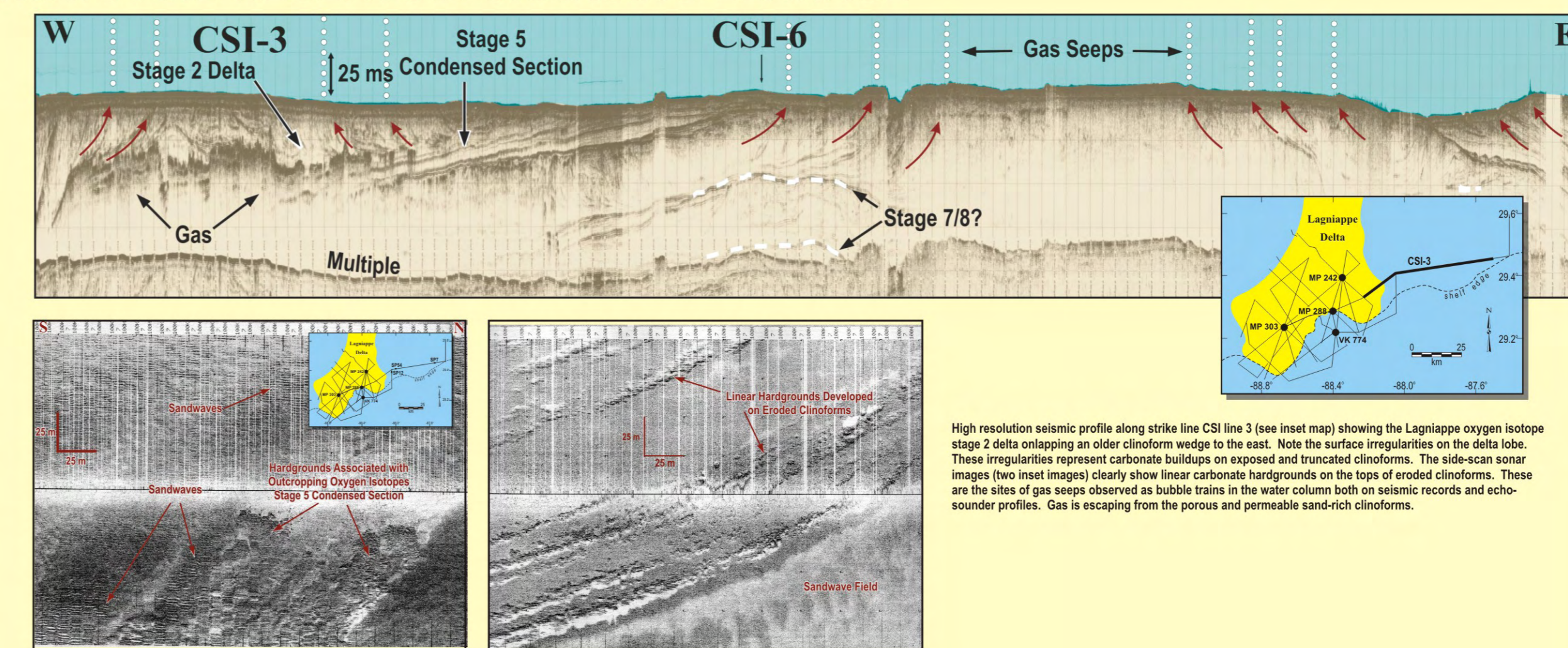
Richard H. Fillon
Earth Studies Associates
3730 Rue Nicole
New Orleans, Louisiana 70131 USA

Harry H. Roberts
Coastal Studies Institute
Louisiana State University
Baton Rouge, Louisiana 70803-7257 USA

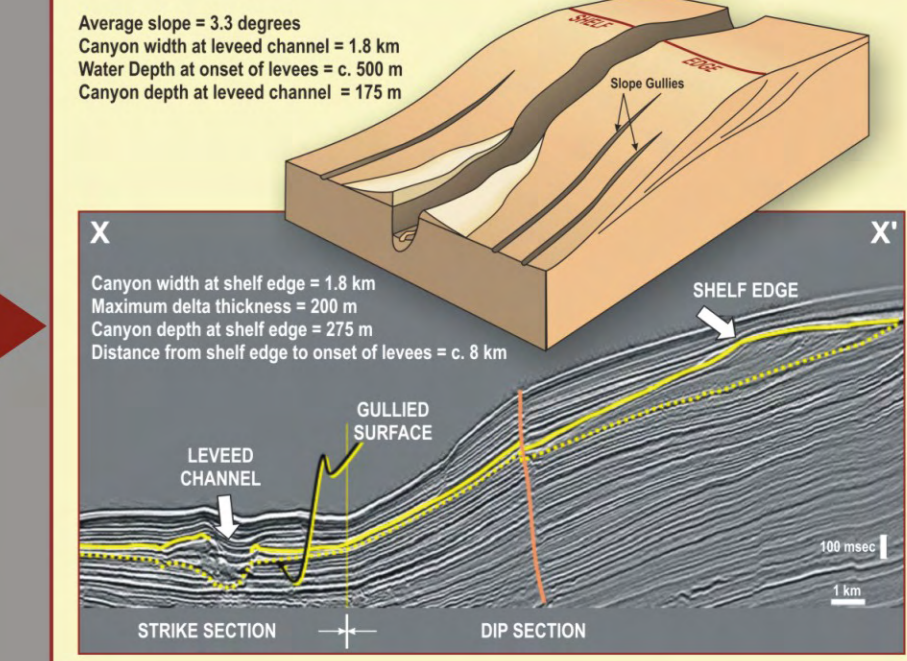
MIGRATORY PATHWAYS AND RESERVOIR CHARGING-LEAKAGE



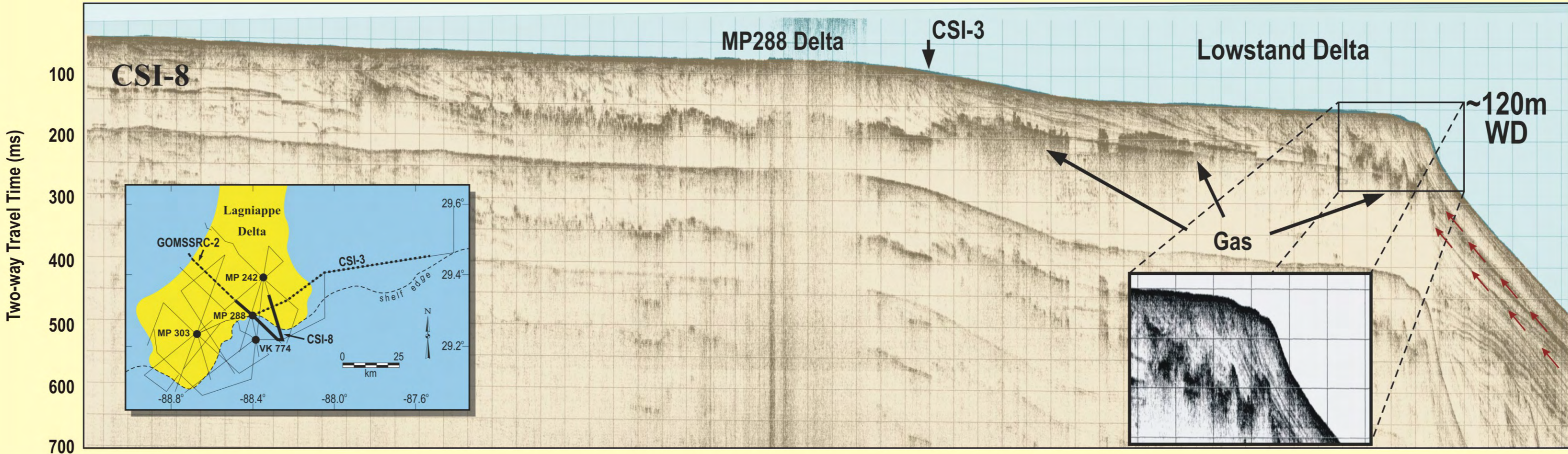
This regional seismic profile demonstrates the thin connective beds (turbidite deposits) between the up-dip shelf-edge delta and a down-dip channel-levee system. The inset figure shows a seismic profile across the Stage 2 Lagniappe delta at the present shelf-edge and an underlying Stage 8 delta. Corals through both deltas indicate sand-rich clinoforms. Potential migration pathways up the heterolithic clinoform toes are illustrated.



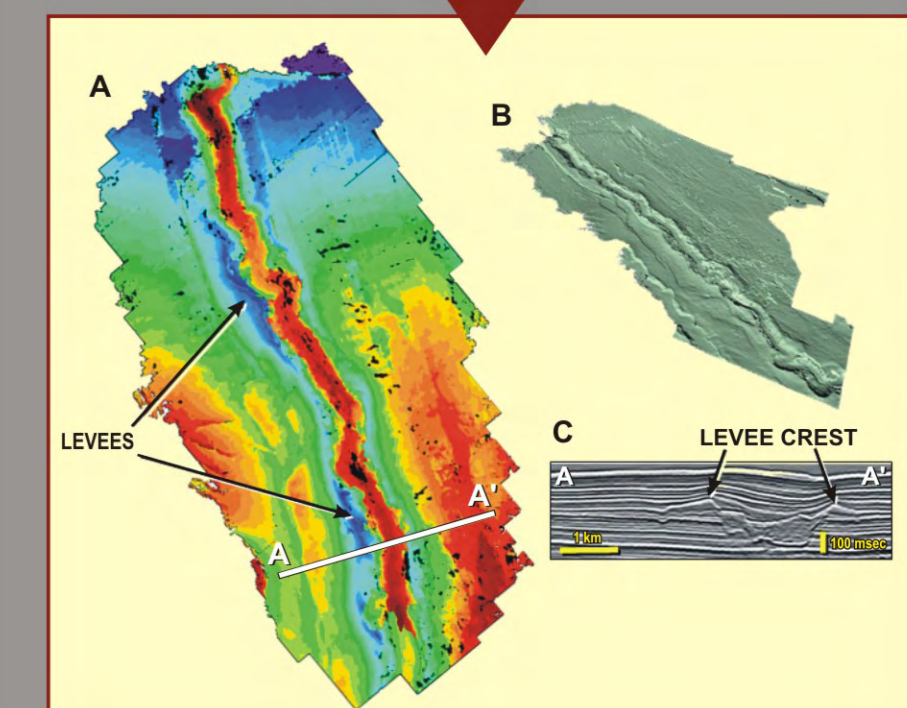
High resolution seismic profile along strike line CSI-3 (see inset map) showing the Lagniappe oxygen isotope stage 2 delta overlapping an older clinoform wedge to the east. Note the surface irregularities on the delta lobe. These irregularities represent carbonate buildups on exposed and truncated clinoforms. The side-scan sonar images (two inset images) clearly show linear carbonate hardgrounds on the tops of eroded clinoforms. These are the sites of gas seeps observed as bubble trains in the water column both on seismic records and echo-sounder profiles. Gas is escaping from the porous and permeable sand-rich tops.



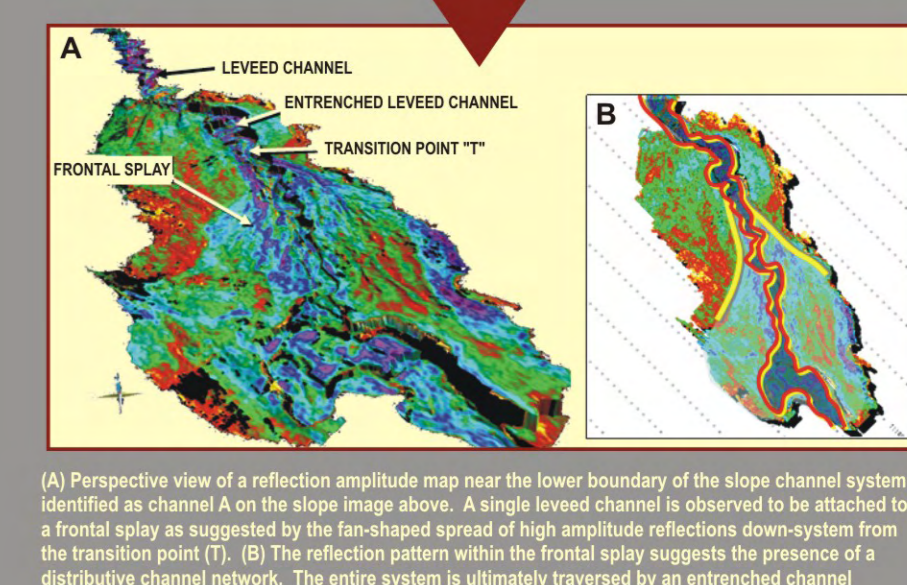
In this figure a dip-oriented seismic reflection profile from a buried shelf-edge delta, defined as a clinoform wedge is linked to its associated down-dip leveled channel (channel A on adjacent slope image). This relationship is common along the northeastern Gulf of Mexico continental margin. The inset is a schematic diagram of a shelf-edge delta, canyon-slope channel, down-dip channel-levee complex, and slope gullies. The metrics associated with this diagram are typical of delta-to-leveed channel systems along the northeastern Gulf of Mexico shelf-edge transition (modified from Posamentier, 2003).



High-resolution seismic lines CSI line 8 and GOMSSRC line 2 illustrate truncated clinoforms at a subsea elevation consistent with the generally accepted ~120 m for sea level at the LGM. Stratigraphic relationships, in CSI line 8, indicate that the clinoforms at approximately ~120 m postdate the shallower and upslope clinoform set dated at ca. 19 ka. Note the high amplitude reflection patterns in the lower parts of the clinoforms. These patterns are interpreted as the presence of bubble phase gas.



(A) Isobath map of the levees associated with slope channel B as shown on the above slope image. Note the low sinusoidal of the channel that likely was associated with the formation of these levees. Levee thickness reaches a maximum of 80 m. (B) Levee tops are illustrated in this perspective view. (C) This transverse seismic reflection cross section clearly illustrates a buried channel-levee morphology (modified from Posamentier, 2003).



(A) Perspective view of a reflection amplitude map near the lower boundary of the slope channel system identified as channel A on the slope image above. A single leveed channel is observed to be attached to a frontal splay as suggested by the fan-shaped spread of high amplitude reflections down-slope from the transition point (T). (B) The reflection pattern within the frontal splay suggests the presence of a distributive channel network. The entire system is ultimately traversed by an entrenched channel (modified from Posamentier, 2003).